Bound-to-continuum Approach for keV Nucleon Radiative Capture Reactions

Minh-Loc BUI

Center for Exotic Nuclear Studies
Institute for Basic Science, Daejeon, Korea

March 16, 2022

Nucleon Radiative Capture Reactions in the CNO cycle

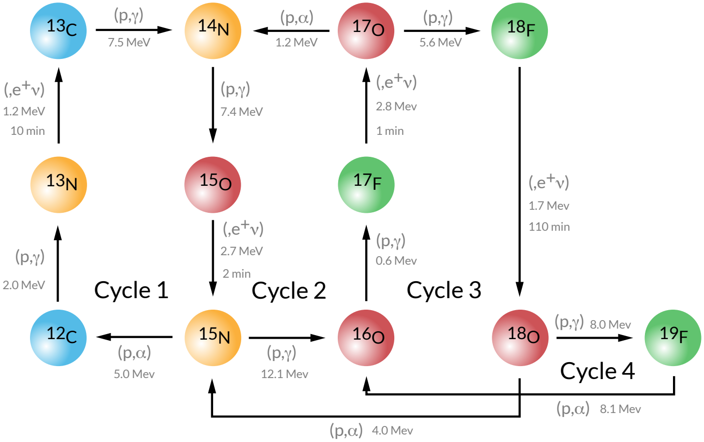

CNO: $T_9 < 0.2$

Figure 1: CNO nucleosynthesis cycle. http://cococubed.asu.edu.

The *pp* chain and the CNO cycle

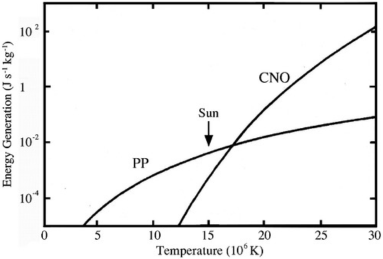

Figure 2: pp chain, and CNO cycle.

Our Sun: The pp chain dominates. Alien's sun: The CNO dominates. Red-Giant branch stars have an inert helium core surrounded by a shell of hydrogen fusing into helium via a six-stage sequence of nuclear decays and reactions known as the CNO nucleosynthesis cycle at very low energy. At the core, $T_{RGB} = 0.1$ GK ≈ 80 keV [1].

Nuclear reactions in the CNO cycle are at keV energy.

---

[1] 1 keV corresponds to 11.6 million K. $T_{\odot} = 0.015$ GK ≈ 2 keV at the core.

An example

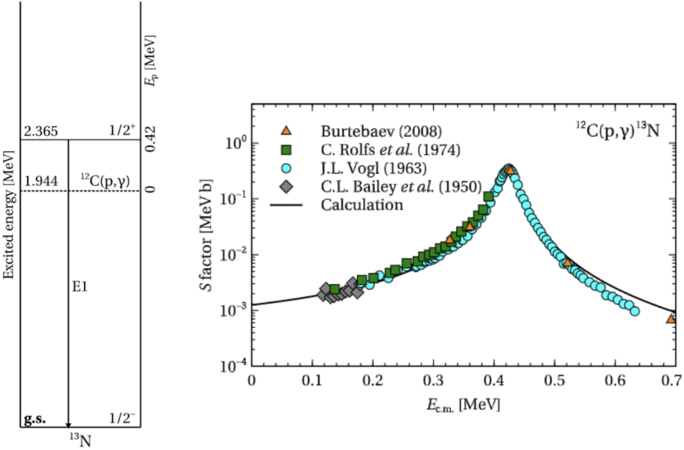

Figure 3: At low energy, there is the resonance at 0.42 MeV corresponding to the $1/2^+$ excited state of ^{13}N at 2.365 MeV. There is the bound-to-bound $E1$ transition to the g.s.. The (p, γ) reaction is a continuum-to-bound transition. The threshold of the reaction is 1.944 MeV.

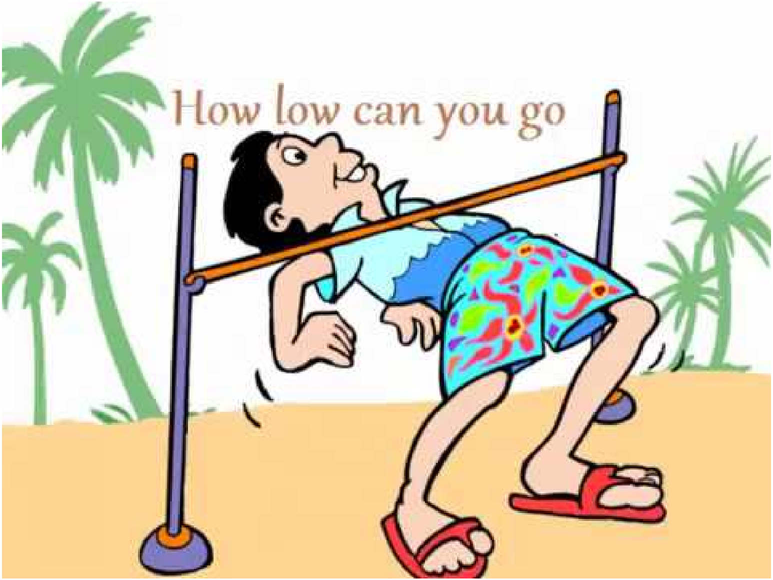

Figure 4: Limbo game. It's about how low the experiment can go.

Outline

- The radiative capture (RC) reactions are the nuclear reactions in which the incident particle (neutron, proton, α, and other light ions) is absorbed by the target nucleus, and the γ radiation is then detected.
  They are important in applied and pure nuclear physics, specially nuclear astrophysics.
- Bound-to-continuum approach is the new approach for the study of RC. It based on the Hartree-Fock single-particle potential for the scattering state.
- The study focuses on light nuclei (carbon, nitrogen, and oxygen) and keV-energy region including zero energy (nuclear astrophysics). The nuclear structure (spectroscopic factor) is also discussed.
- Future perspectives.

Introduction: the Potential Model

There are several models [2]: *R*-matrix theory, microscopic cluster model, **potential model**, and other models...

At very low energies

The astrophysical $\mathcal{S}$-factor: $\mathcal{S}(E) = E \exp(2\pi\eta)\sigma(E)$.

$$\sigma(E) = \frac{4}{3}\frac{e^2}{\hbar}\left(\frac{4}{3}\pi k_\gamma^3\right)\left(\frac{A\tau - Z}{A+1}\right)^2 |\mathcal{M}_{i\to f}(E)|^2, \tag{1}$$

$$\mathcal{M}_{i\to f} = \langle \Psi_f | \mathcal{O}(E1) = rY(\theta,\phi) | \Psi_i \rangle = A \cdot S_F \cdot \mathcal{I}(E). \tag{2}$$

A is the angular-spin coefficient.
S_F is the spectroscopic factor of the final single-particle (s.p.) state!
$\mathcal{I}(E)$ is the radial overlap function

$$\mathcal{I}(E) = \int \varphi_{n_f \ell_f j_f}(r)\, r\, \chi_{\ell_i}(E,r) dr. \tag{3}$$

---

[2] Descouvermont, Front. Astron. Space Sci. **7** (2020) for a review.

RC reactions (p, γ) in PRC 103 (2021)

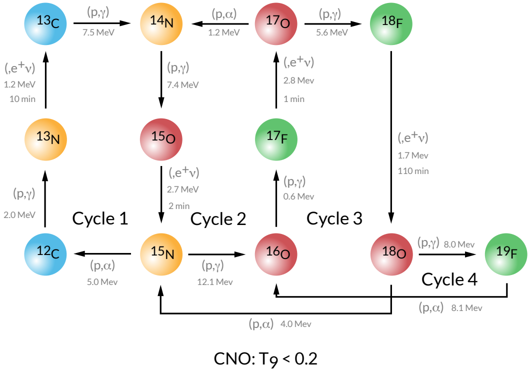

① $^{12}\mathrm{C}(p, \gamma)^{13}\mathrm{N}_{\mathrm{g.s.}}$
② $^{13}\mathrm{C}(p, \gamma)^{14}\mathrm{N}_{\mathrm{g.s.}}$
③ $^{13}\mathrm{C}(p, \gamma)^{14}\mathrm{N}^{*}_{0^{+}}$
④ $^{13}\mathrm{C}(p, \gamma)^{14}\mathrm{N}^{*}_{1^{+}_{2nd}}$
⑤ $^{14}\mathrm{N}(p, \gamma)^{15}\mathrm{O}_{\mathrm{g.s.}}$
⑥ $^{14}\mathrm{N}(p, \gamma)^{15}\mathrm{O}^{*}_{3/2^{-}}$
⑦ $^{16}\mathrm{O}(p, \gamma)^{17}\mathrm{F}_{\mathrm{g.s.}}$
⑧ $^{16}\mathrm{O}(p, \gamma)^{17}\mathrm{F}^{*}_{1/2^{-}}$

Figure 5: CNO nucleosynthesis cycle. http://cococubed.asu.edu.

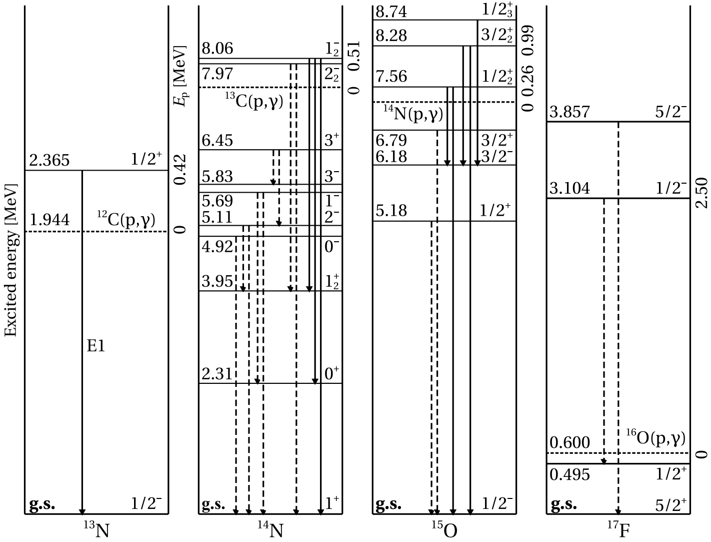

Figure 6: The considered $E1$ transitions are the solid arrows (bound-to-bound transition). The (p,γ) process is the continuum-to-bound transition.

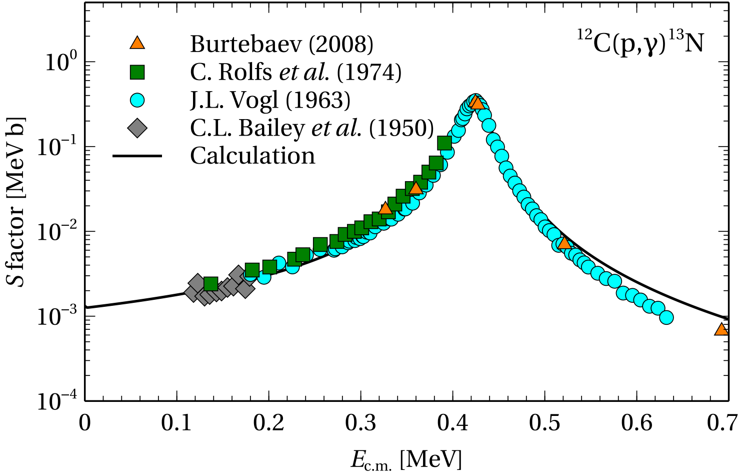

Figure 7: The ongoing experiment of LUNA project (Laboratory for Underground Nuclear Astrophysics).

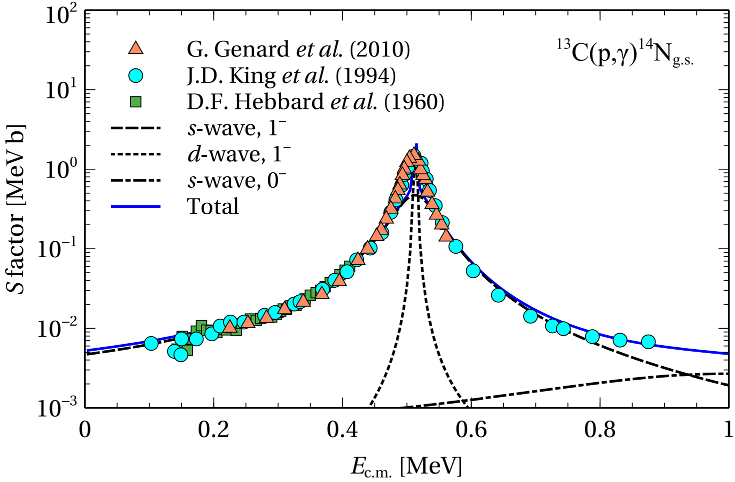

Figure 8: ^{13}C$(p,\gamma)^{14}$N$_{g.s.}$. Note: the narrow resonance caused by the *d*-wave. The tail was lifted by the resonance at 8.78 MeV (LUNA).

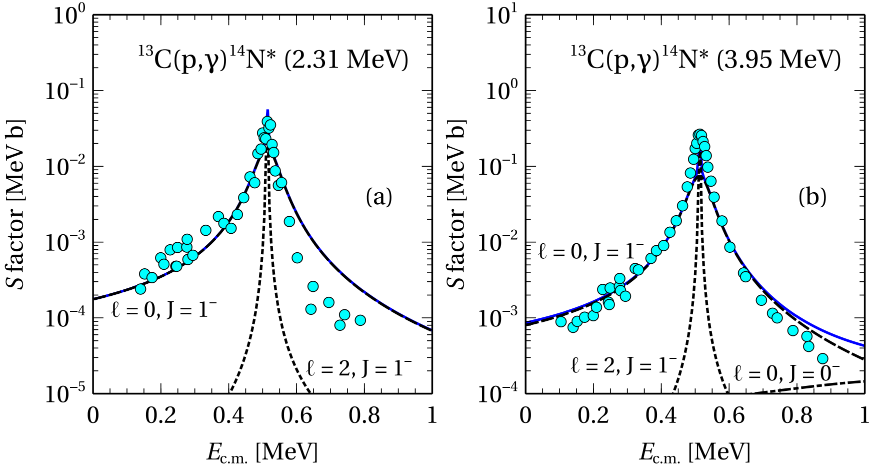

Figure 9: $^{13}C(p, \gamma)^{14}N^*$ to the excited states, at 2.31 (a) and 3.95 MeV (b).

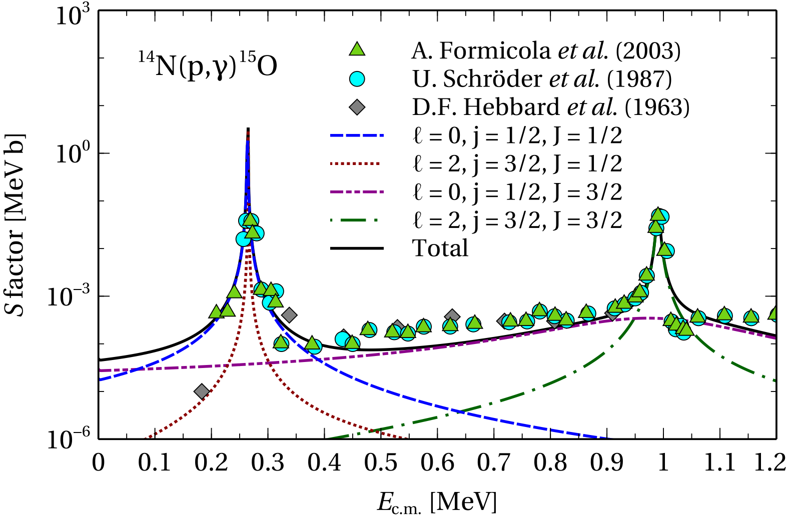

Figure 10: Two resonances. The partial-wave analysis is important.

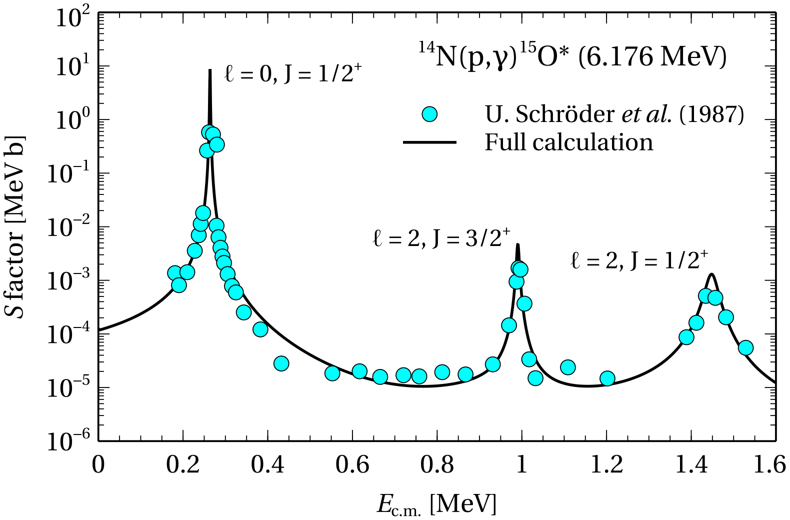

Figure 11: Three resonances. The widths are automatically correct.

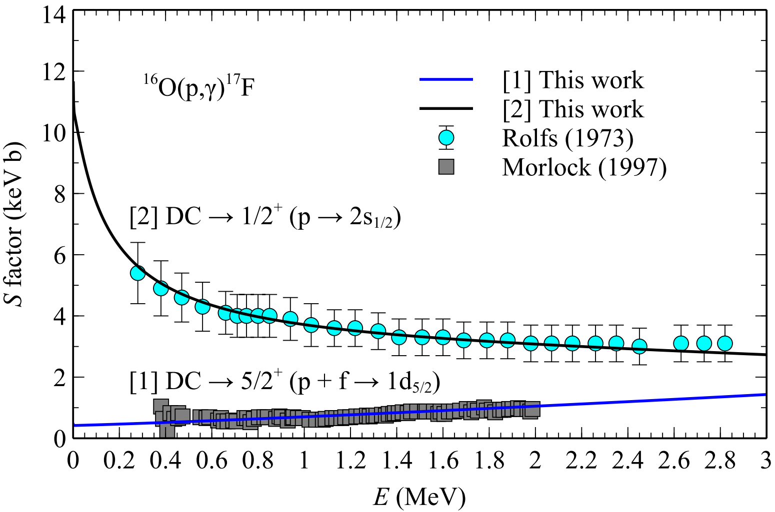

Figure 12: There is no resonance for calibration (not necessary for ^{16}O).

(n, γ) reactions

The (n, γ) is different from the (p, γ) by the Coulomb potential.

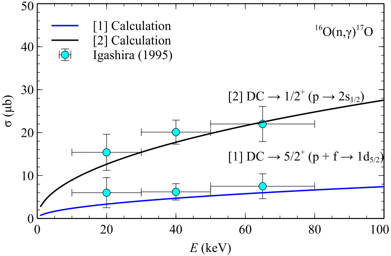

Figure 13: $^{16}O(n, \gamma)^{17}O$.

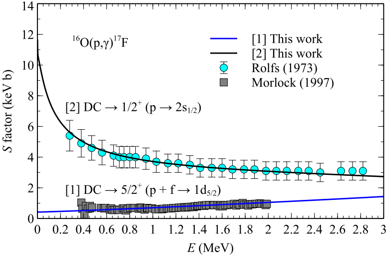

Figure 14: $^{16}O(p, \gamma)^{17}F$.

- Non-resonance reactions.
- The error bar is large.

[PRC 104 (2021)]

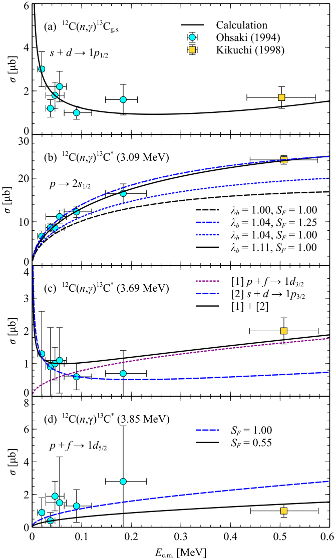

Figure 15: $^{12}C(n,\gamma)^{13}C$

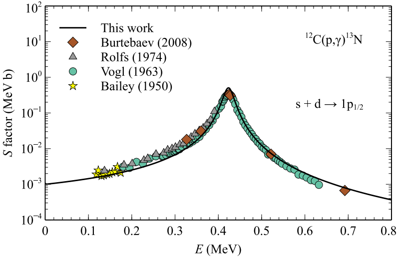

Figure 16: $^{12}C(p,\gamma)^{13}N$

The resonance is valuable not only for (p,γ) but also for (n,γ).
The data point at $0.5-1.0$ MeV is also essential.

Table 1: φ_α is the Skyrme HF value, e_s is the nucleon separation energy used in our calculation, and $S^{exp}_{p(n)} = -Q + E_x$ is from experiments.

Reaction	J_f^π	χ_{l_i}	φ_α	ϵ_α	$S^{exp}_{p(n)}$	e_s	λ_b	S_F
$^{16}\mathrm{O}(p,\gamma)^{17}\mathrm{F}$	$\frac{5}{2}^+$	p, f	$1d_{\frac{5}{2}}$	-3.57	-0.60	-0.60	0.88	1.00
$^{16}\mathrm{O}(p,\gamma)^{17}\mathrm{F}^*$	$\frac{1}{2}^+$	p	$2s_{\frac{1}{2}}$	-0.97	-0.11	-0.11	0.95	1.00
$^{16}\mathrm{O}(n,\gamma)^{17}\mathrm{O}$	$\frac{5}{2}^+$	p, f	$1d_{\frac{5}{2}}$	-6.75	-4.14	-4.14	0.90	1.00
$^{16}\mathrm{O}(n,\gamma)^{17}\mathrm{O}^*$	$\frac{1}{2}^+$	p	$2s_{\frac{1}{2}}$	-3.89	-3.27	-3.89	1.00	1.00
$^{12}\mathrm{C}(p,\gamma)^{13}\mathrm{N}$	$\frac{1}{2}^-$	s, d	$1p_{\frac{1}{2}}$	-6.85	-1.94	-1.94	0.81	0.20
$^{12}\mathrm{C}(n,\gamma)^{13}\mathrm{C}$	$\frac{1}{2}^-$	s, d	$1p_{\frac{1}{2}}$	-9.42	-4.95	-4.95	0.83	0.45
$^{12}\mathrm{C}(n,\gamma)^{13}\mathrm{C}^*$	$\frac{1}{2}^+$	p	$2s_{\frac{1}{2}}$	-1.25	-1.86	-3.02	1.11	1.00
$^{12}\mathrm{C}(n,\gamma)^{13}\mathrm{C}^*$	$\frac{3}{2}^-$	s, d	$1p_{\frac{3}{2}}$	-16.85	-1.26	-1.26	0.45	0.25
		p, f	$1d_{\frac{3}{2}}$	0.97	-1.26	-1.26	1.30	0.95
$^{12}\mathrm{C}(n,\gamma)^{13}\mathrm{C}^*$	$\frac{5}{2}^+$	p, f	$1d_{\frac{5}{2}}$	-2.30	-1.09	-1.09	0.94	0.55

$\lambda_s = 1.0, 1.02$ for ^{16}O and ^{12}C.

Table 2: The S_F from [Bertulani (2010) [1]], and [NACRE [2]].

No.	Reactions	J^π	ℓ	λ_c	$J'^{\pi'}$	α	λ_b	S_F	S_F [1]	S_F [2]
1	$^{12}\mathrm{C}(p,\gamma)^{13}\mathrm{N}$	$1/2^+$	s	1.15	$1/2^-$	$1p_{1/2}$	0.83	0.36	0.35	0.33
2	$^{13}\mathrm{C}(p,\gamma)^{14}\mathrm{N}$	1^-	s	1.03	1^+	$1p_{1/2}$	0.97	0.23	0.15	0.28
3		1^-	d	1.22	1^+	$1p_{1/2}$	0.97	0.23	-	-
4	$^{13}\mathrm{C}(p,\gamma)^{14}\mathrm{N}^*_{0^+}$	1^-	s	1.03	0^+	$1p_{1/2}$	0.88	0.04	-	0.027
5		1^-	d	1.22	0^+	$1p_{1/2}$	0.88	7×10^{-3}	-	-
6	$^{13}\mathrm{C}(p,\gamma)^{14}\mathrm{N}^*_{1_2^+}$	1^-	s	1.03	1^+	$1p_{1/2}$	0.82	0.16	-	0.28
7		1^-	d	1.22	1^+	$1p_{1/2}$	0.82	0.16	-	-
8	$^{14}\mathrm{N}(p,\gamma)^{15}\mathrm{O}$	$1/2^+$	s	1.08	$1/2^-$	$1p_{1/2}$	0.97	2×10^{-3}	-	3.5×10^{-5}
9		$1/2^+$	d	1.23	$1/2^-$	$1p_{1/2}$	0.97	2×10^{-3}	-	-
10		$3/2^+$	d	1.19	$1/2^-$	$1p_{1/2}$	0.97	5×10^{-3}	-	3.4×10^{-5}
11	$^{14}\mathrm{N}(p,\gamma)^{15}\mathrm{O}^*_{3/2^-}$	$1/2^+$	s	1.08	$3/2^-$	$1p_{1/2}$	0.73	0.08	-	2.4×10^{-5}
12		$3/2^+$	d	1.19	$3/2^-$	$1p_{1/2}$	0.73	0.02	-	1.7×10^{-5}
13		$1/2^+$	d	1.17	$3/2^-$	$1p_{1/2}$	0.73	0.35	-	5.0×10^{-3}
14	$^{16}\mathrm{O}(p,\gamma)^{17}\mathrm{F}$	$3/2^-$	p	1.00	$5/2^+$	$1d_{5/2}$	1.03	1.00	0.90	-
15	$^{16}\mathrm{O}(p,\gamma)^{17}\mathrm{F}^*_{1/2^-}$	$3/2^-$	p	1.00	$1/2^+$	$2s_{1/2}$	1.05	1.00	1.00	-

Conclusions and future perspectives

1. The RC reactions have been concerned with astrophysical aspects, but they can be a useful tool in nuclear spectroscopy [**Rolfs, NPA 217 (1973)**].
2. The Skyrme HF calculation is the starting point. Strictly speaking, the pairing and deformation should be taken into account in the calculation (not in the case of ^{16}O).
3. The bound-to-continuum approach is very promising for the low-energy nuclear reactions, first of all, the OMP.

Future perspectives

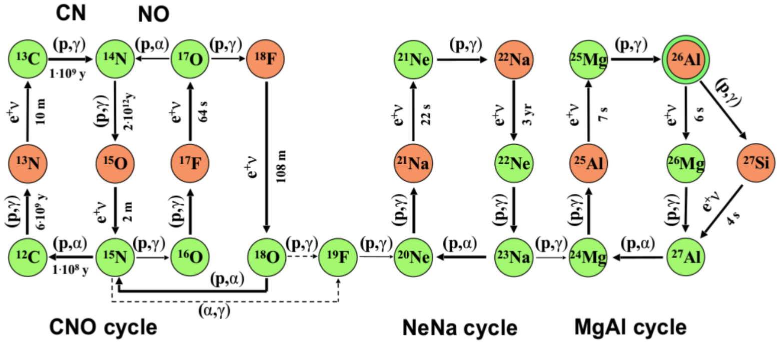

Figure 17: There are so many RC reactions in nuclear astrophysics. A reliable theory model is very useful.

Thank you for your attention!